EFFECT OF THE BONDING TIME ON THE MICROSTRUCTURE AND MECHANICAL PROPERTIES OF A TRANSIENT-LIQUID-PHASE BONDED IN718 USING A Ni-Cr-B FILLER ALLOY

VPLIV ČASA SPAJANJA NA MIKROSTRUKTURO IN MEHANSKE LASTNOSTI SPOJA S PREHODNO TEKOČO FAZO PRI SPAJANJU IN718 Z UPORABO ZLITINE Ni-Cr-B ZA SPAJANJE

Majid Pouranvari, Ali Ekrami, Amir Hossein Kokabi

Department of Materials Science and Engineering, Sharif University of Technology, 11365-11155 Tehran, Iran
mpouranvari@yahoo.com, mpouranvari@mehr.sharif.ir

The paper aims at addressing the effect of the bonding time on the metallurgical and mechanical properties of a transient-liquid-phase (TLP) bonded IN718 nickel-based superalloy using an Ni-15.2Cr-4B (%) amorphous filler alloy. The results showed that after a partial isothermal solidification, the residual liquid in the joint centerline transformed, during the cooling, to non-equilibrium eutectic-type microconstituents composed of Ni-rich boride, Cr-rich boride and eutectic γ-solid solution phase. The complete isothermal solidification which resulted in a formation of an intermetallic-free joint centerline occurred after a holding period 40 min at the bonding temperature of 1100 °C. An increase in the bonding time improved the joint shear strength due to a decrease in the width of the eutectic-type microconstituents in the joint centerline.

Keywords: transient-liquid-phase bonding, superalloy, solidification, mechanical properties

Članek obravnava vpliv časa spajanja na metalurške in mehanske lastnosti nikljeve superzlitine IN718, spojene s prehodno tekočo fazo (TLP) in z uporabo Ni-15,2Cr-4B (%) amorfnega polnila. Rezultati kažejo, da se po delnem izotermnem strjevanju preostala talina v sredini spoja pretvori pri ohlajanju v neravnotežno evtektičnega tipa, ki jo sestavljajo z Ni bogati boridi, s Cr bogati boridi in evtektična γ- trdna raztopina. Popolno izotermno strjevanje je bilo doseženo po 40 min zadrževanja pri 1100 °C, pri čemer je nastala sredica spoja brez intermetalnih zlitin. Podaljšanje časa spajanja je izboljšalo strižno trdnost spoja zaradi zmanjšanja širine sestavine evtektičnega tipa v sredini spoja.

Ključne besede: spajanje s prehodno tekočo fazo, superzlitina, strjevanje, mehanske lastnosti

1 INTRODUCTION

Nickel-based superalloys are extensively used in the modern industry due to their excellent high-temperature tensile strength, stress rupture and creep properties, fatigue strength, oxidation and corrosion resistance, and microstructural stability at elevated temperatures.[1–3] The superalloy IN718 is one of the workhorse materials being extensively used in critical aero-engines and space applications for high-temperature, creep-resistant applications, nuclear power plants and petrochemical industry.[4] The strength of IN718 is governed by both the solid-solution and precipitation-hardening mechanisms. While both ordered face-centered-cubic (FCC) γ'-Ni$_3$(Al,Ti) and metastable ordered body-centered-tetragonal (BCT) γ''-Ni$_3$Nb precipitates are formed during an aging cycle of the alloy, the predominant contribution to the precipitation hardening is provided by the latter.[5]

Fusion welding and brazing are two main repairing/joining techniques for superalloys that have been commonly applied in industry.[6] Conventionally, high temperature brazing, using nickel-based filler alloys, is extensively used as a standard repair/regeneration tech-

nique for superalloy components.[7,8] In order to lower the liquidus temperature of nickel-based superalloys and increase the fluidity of the braze, melting point depressants (MPD) and modifiers such as phosphorus, silicon and boron are added to the braze alloy. However, these elements are incorporated into the intermetallic phases such as borides, silicides and phosphides during a non-equilibrium eutectic-type solidification of the liquid phase during the cooling stage of the brazing process.[9,10] The presence of the intermetallic phases in a brazed joint's centerline is known to detrimentally affect the performance of the joint in several ways:

1. Reducing the mechanical properties.[11–14]
2. Lowering the re-melting temperature and service temperature of a brazed component due to the segregation of the melting-point depressants into a low melting-point eutectic.[15]
3. Reducing the corrosion and oxidation resistance of the brazed component.[15]

While the sluggish kinetics of the γ'' precipitation makes the IN718 welds free of strain-age cracking,[16] the welding of IN718 suffers from certain problems including:

1. Microfissuring and liquation cracking in the HAZ.[4,17]

2. The segregation of Nb during the non-equilibrium solidification of the fusion zone and the consequent formation of the Nb-rich Laves phase.[4,18,19]

Transient-liquid-phase bonding or diffusion brazing is considered to be the preferred repairing/joining process for the nickel-based superalloys,[6,15,20–24] which is a hybrid process, combining beneficial features of the liquid-phase bonding and the solid-state bonding. In general, it is considered that there are three distinct stages during the diffusion brazing, namely: the base-metal dissolution, the isothermal solidification and the solid-state homogenization.[21] Combining isothermal solidification with the subsequent solid-state homogenization treatment, offers a possibility of producing the bonds that are chemically almost identical to the parent material and have no discernable microstructural discontinuity at the bond line.[15,21]

Despite an extensive application of IN718 in various industries, there is only a limited number of published works[12] on the diffusion brazing of this superalloy. There have been some modeling efforts regarding the isothermal solidification time for the TLP bonding of a wrought IN718 alloy using a Ni-Cr-Si-Fe-B filler alloy.[12] In addition, there is only limited information regarding the microstructure development and mechanical properties during a TLP bonding of this superalloy. Therefore, this paper aims at investigating the metallurgy of diffusion brazing of a cast IN718 nickel-based superalloy using a Ni-Cr-B filler alloy.

2 EXPERIMENTAL PROCEDURE

A cast IN718 nickel-based superalloy was used as the base metal in this investigation. A 50 μm thick amorphous Ni-Cr-B (MBF80) filler alloy was used as the interlayer for the TLP bonding. The chemical composition of the base metal and the filler metal is given in **Table 1**.

10 mm × 5 mm × 5 mm coupons were sectioned from the base metal using an electro-discharge machine. Thereafter, in order to remove the oxide layer, the contacting surfaces were grounded using 600-grade SiC paper and then ultrasonically cleaned in an acetone bath. The interlayer was then inserted between two base-metal coupons. A Cr-Mo steel fixture was used to fix the coupons in order to hold the sandwich assembly and reduce the metal flow during the TLP operation. No external pressure was applied at the bond line. The bonding operation was carried out in a vacuum furnace under a vacuum of approximately 1.33×10^{-5} mbar. The bonding temperature was selected as 1100 °C. The bonding time was varied from 10 min to 40 min.

The bonded specimens were sectioned perpendicularly to the bond and then microstructural observations were made on the cross-sections of the specimens using an optical microscope and a field emission scanning electron microscope (FESEM). For the microstructural examinations, specimens were etched using 10 mL of HNO_3, 10 mL of $C_2H_4O_2$, and 15 mL of HCl. Semi-quantitative chemical analyses of the phases formed in the centerline of the bond region and adjacent to the base metal were conducted using a JEOL 5900 FESEM equipped with an ultra-thin-window Oxford Energy Dispersive X-ray Spectrometer (EDS). The element distribution across the joint region was analyzed using a JEOL JXA-8900R electron probe X-ray microanalyzer equipped with line-scan Wavelength-Dispersive Spectrometry (WDS).

A microhardness test was used to determine the joint-region hardness profile. The test was conducted on the sample cross-sections using a 10 g load on a Buehler microhardness tester. To evaluate the mechanical strength of the TLP bonds, the shear test was used instead of the tensile test. The tensile test is not strict to the bond line. Indeed, a minimum amount of the bond line is oriented on the plane experiencing the maximum resolved shear stress (i.e., the plane is oriented at 45° to
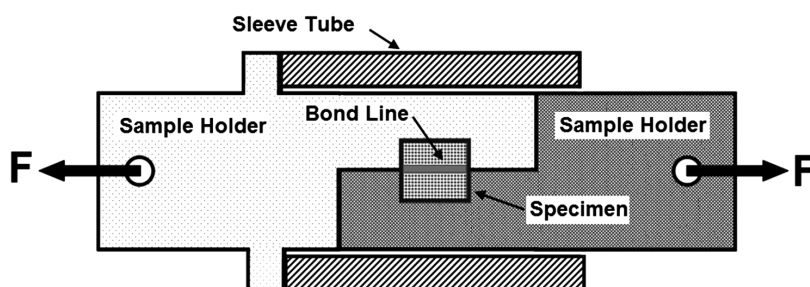
Figure 1: Schematic diagram of a shear-test fixture
Slika 1: Shematski prikaz pritrditve pri strižnem preizkusu

Table 1: Chemical compositions (amount fraction, $\varphi/\%$) of the base metal and interlayer
Tabela 1: Kemijska sestava (množinski delež, $\varphi/\%$) osnovne kovine in vmesnega sloja

	Ni	Cr	Fe	Nb	Mo	Ti	Al	B
IN718	Balance	20.07	18.56	2.75	1.99	1.11	0.86	0.037
Interlayer	Balance	14.34	–	–	–	–	–	18.15

the tensile axis).[25] Therefore, it can be deduced that a tensile testing of a TLP bond with a thin interlayer (i.e., 50 μm) does not effectively test the bond line. Therefore, a fixture was designed for the shear testing (**Figure 1**). The designed fixture subjects a sample to a pure shear stress at the bond line. A room-temperature shear test was performed employing an Instron tensile machine with a cross-head speed of 2 mm/min. The edge effects were eliminated by machining before the shear test.

3 RESULTS AND DISCUSSION

3.1 Microstructure and hardness characteristics in a partially isothermal solidified bond

Figures 2a and **b** show optical microscopy images of the bonds made at 1100 °C for 10 min indicating three distinct microstructural zones in the bond region:

(i) Isothermally solidified zone (ISZ):

This zone is formed due to an interdiffusion-induced compositional change.[20] A typical compositional analysis of ISZ is given in **Table 2**. The microstructure of this zone consisted of a proeutectic Ni-rich γ solid-solution phase and it is free of the intermetallic phase. According to **Table 2**, this zone contains certain amounts of Nb, Mo, Al and Ti that were not present in the initial composition of the filler alloy. This indicates a dissolution of the base metal during the bonding process. The diffusion of boron (B) from the liquid phase into the base metal increases the liquidus temperature of the liquid phase. Once the liquidus temperature reaches the bonding temperature, the liquid re-solidifies during the holding time at the bonding temperature (i.e., the isothermal solidification starts). Due to the absence of the solute rejection at the solid/liquid interface during the isothermal solidification under equilibrium condition, the only solid phase that forms is the solid-solution phase and the formation of the other phases is basically prevented.[14]

(ii) Athermally solidified zone (ASZ):

This zone is formed due to an insufficient time for the completion of isothermal solidification. The microstructure of ASZ consists of the microconstituents with a eutectic-like morphology and is made up of three distinct phases (**Figures 2c**, **e**, **f**). The phases in ASZ are marked as X, Y and Z. Their SEM-EDS spectra are shown in
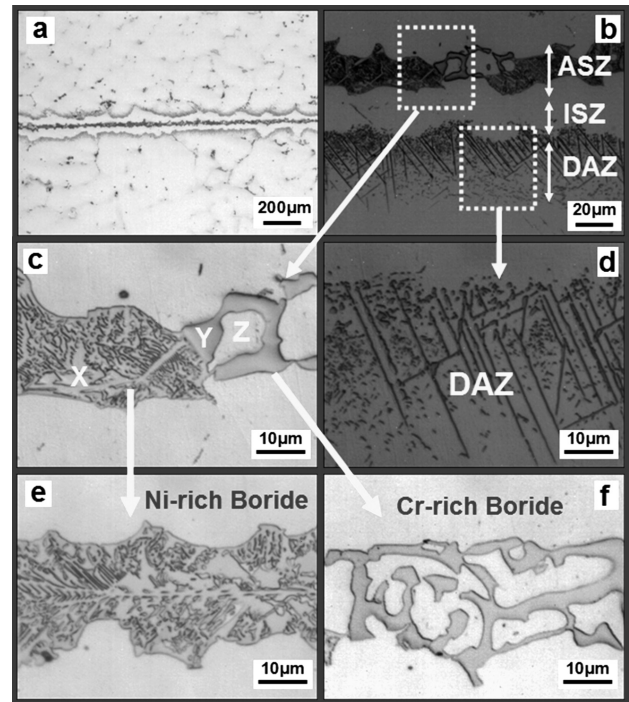
Figure 2: Microstructure of TLP bonded IN718 at 1100 °C for 10 min: a) and b) overview of the joint region indicating three distinct microstructural zones including athermal solidification zone (ASZ), isothermal solidification zone (ISZ) and diffusion affected zone (DAZ); c) a magnified micrograph of eutectic microconstituents in ASZ; d) secondary precipitates in DAZ; e) a magnified view of Ni-rich boride; f) a magnified view of Cr-rich boride
Slika 2: Mikrostruktura TLP-spoja IN718 pri 1100 °C, 10 min: a) in b) pregled območja spoja, ki kaže tri ločena področja, vključno z atermičnim področjem strjevanja (ASZ), področje izotermičnega strjevanja (ISZ) in difuzijsko vplivanega področja (DAZ), c) povečan posnetek evtektika v ASZ, d) sekundarni izločki v DAZ, e) povečan posnetek z Ni bogatih boridov, f) povečan posnetek s Cr bogatih boridov

Figure 3. Typical compositional analyses of the X, Y and Z are given in **Table 2**. The EDS analyses suggest that X is Ni-rich boride (**Figure 2e**). **Figure 4** shows an X-ray elemental map of the phase marked as Y. According to **Figures 3b** and **4**, this intermetallic phase is Cr-rich boride (**Figure 2f**) which is also rich in Mo and Nb. The phase marked as Z is a Ni-rich solid solution formed as a part of the eutectic reaction.

Indeed, the presence of an intermetallic phase in the joint centerline indicates that the bonding time of 10 min

Table 2: Chemical compositions (amount fraction, φ/%) of different metallic constituents for various phases observed in the brazed affected zone
Tabela 2: Kemijska sestava (množinski delež, φ/%) različnih kovinskih sestavin različnih faz, opaženih v območju vpliva spajkanja

		Ni	Cr	Fe	Mo	Nb	Al	Ti
ASZ	Ni-rich boride*	74.93	13.19	3.12	–	6.70	–	2.06
	Cr-rich boride*	6.71	55.64	3.29	12.87	20.71	–	0.78
	γ eutectic	68.54	17.49	5.5	0.45	6.31	0.38	1.33
DAZ	Needle-like precipitates*	56.44	22.34	11.67	4.82	2.98	0.92	0.83
	Adjacent γ matrix	66.54	13.43	15.54	1.74	1.32	0.71	0.72
ISZ	Solid solution	74.53	18.22	4.57	0.69	0.88	0.60	0.51

*Boron could be detected with EDS in this phase, but light elements could not be quantified due to the inability of the EDS system
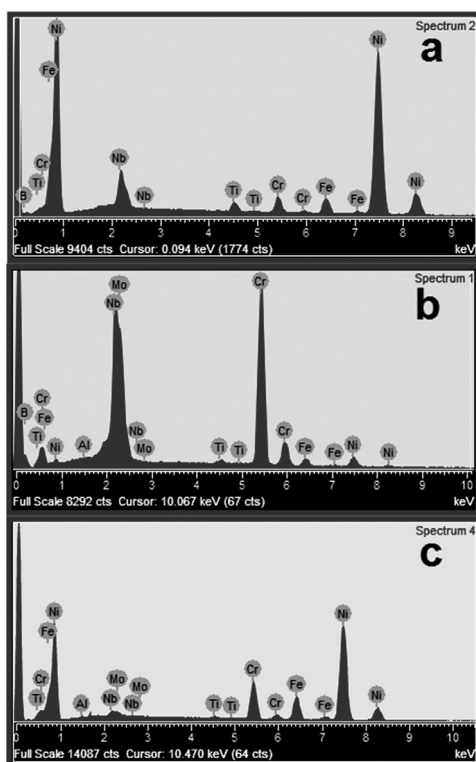
Figure 3: SEM-EDS spectra of: a) Ni-rich boride, b) Cr-rich boride and c) eutectic γ solution
Slika 3: SEM-EDS-spektri: a) z Ni bogati boridi, b) s Cr bogati boridi in c) evtektična γ-raztopina

boride, are formed by the eutectic-type solidification reactions during the cooling, due to an insufficient holding time for a complete isothermal solidification during the bonding.

(iii) Diffusion affected zone (DAZ):

This zone consists of the second-phase particles with two different morphologies: the particles with a blocky morphology and the particles with a needle-like morphology (**Figure 2d**). **Table 2** presents the compositional analyses of the precipitates and the adjacent γ matrix. **Figure 5** shows an X-ray line-scan across some needle-like precipitates in DAZ indicating a partitioning tendency of various elements that are present in the particles compared to that of the adjacent austenitic γ matrix. According to **Table 2** and **Figure 5**, the precipitates are enriched with Cr, Mo, Nb, and B, while they are lean in Fe and Ni. Therefore, this confirms that these secondary phases are Cr-Mo-Nb-based borides.

The morphology of these precipitates suggests that they are not formed during the solidification. The formation of boride precipitates in DAZ is directly associated with the B diffusion out of the liquid into the base metal during the bonding process. Considering the fact that the isothermal solidification is controlled by the diffusion of B into BM, a formation of boride precipitates in DAZ is possible. Due to the diffusion of B into BM, a B-containing alloy is formed in a narrow region in the substrate zone adjacent to ISZ. The solubility of B in this alloy is

is not sufficient for the completion of isothermal solidification. This suggests that there was an amount of the residual liquid in the joint gap after holding the sample at 1100 °C for 10 min. Therefore, the solidification of the residual liquid occurred during the cooling. The segregation of the solute elements is the key feature of the athermal solidification. A very low solubility of B in Ni (amount fractions: 0.3 % according to the binary Ni-B equilibrium phase diagram[26]) and a very low partition coefficient of B in Ni ($\approx$0.008 according to the Ni-B binary phase diagram[26]) lead to a rejection of B into the adjacent melt. A continuous solute enrichment of the liquid could make B exceed the solubility limit of the solute in the γ phase. Then, the secondary solidification constituents (i.e., intermetallic phases) are formed. Ohsasa et al.[27] modeled the solidification behavior of the residual liquid phase during the TLP bonding of Ni/Ni-Cr-B/Ni using the Scheil simulation. They reported that the solidification of the liquid phase started with a formation of the Ni-rich γ solid solution as the primary phase, followed by a eutectic reaction of Ni_3B and the γ solid solution at 1042 °C. The solidification process is terminated by a formation of the ternary eutectic-reaction microconstituents of the γ solid solution, Ni_3B and CrB at 997 °C. Therefore, it can be concluded that the centerline eutectic-like microconstituents observed in the present work, consisting of γ, Bi-rich boride and Cr-rich

Figure 4: X-ray elemental map of Cr-rich boride in ASZ showing that the intermetallic phase is rich in Cr, Mo and Nb and lean in Fe and Ni compared to the surrounding γ solid-solution matrix
Slika 4: Rentgenski posnetek razporeditve s Cr bogatih boridov v ASZ kaže, da so intermetalne faze obogatene s Cr, Mo in Nb, ni pa Fe in Ni v primerjavi z γ-trdno raztopino osnove
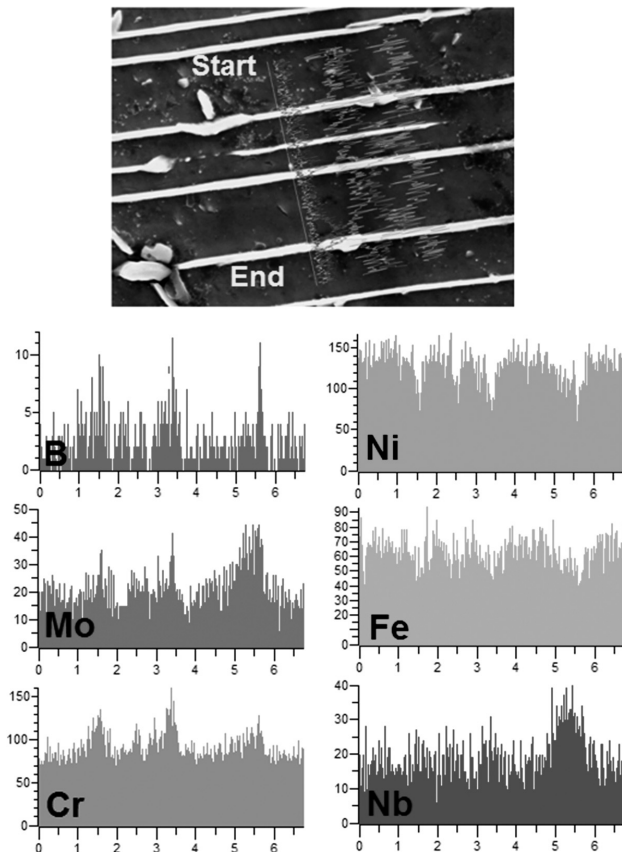
Figure 5: X-ray line scan across the DAZ precipitates showing the partitioning tendency of the elements between the precipitates and the matrix

Slika 5: Rentgenska linijska analiza preko izločkov v DAZ, ki kaže tendenco različnega razporejanja elementov med izločki in osnovo
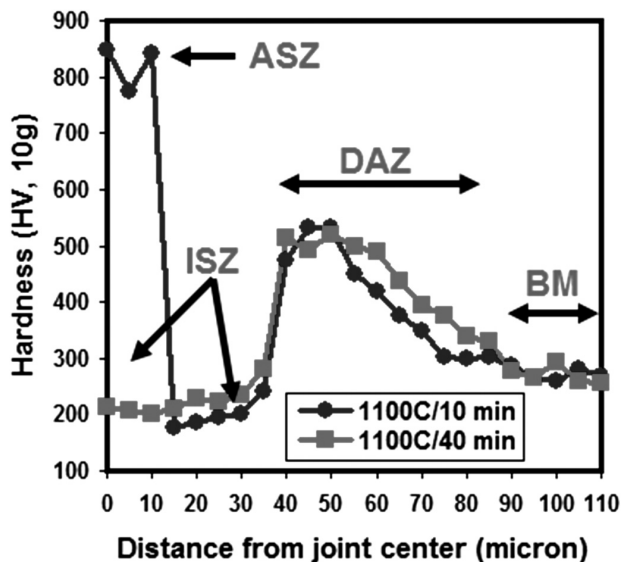
Figure 6: Hardness distribution across the bond region after a partial isothermal solidification at 1100 °C for 10 min and after a complete isothermal solidification at 1100 °C for 40 min

Slika 6: Potek trdote preko spoja po delnem izotermnem strjevanju pri 1100 °C po 10 min ter po popolnem izotermnem strjevanju pri 1100 °C po 40 min

limited. This fact coupled with the presence of Cr, Mo and Nb in the matrix, which are strong boride formers, can explain the formation of the Cr-Mo-Nb-rich precipitates. Gale and Wallach[28] provided the some evidence confirming that these precipitates are formed at the bonding temperature not during the cooling.

The hardness profile across the joint region is a quantitative measurement of the mechanical properties of different zones in the joint region. The hardness profile is a good indicator of the bond microstructure and can be used to assess the effect of the secondary-phase precipitates on mechanical properties.[13] **Figure 6** shows the hardness profile of this bond indicating four distinct zones: Region I corresponds to ASZ. The average hardness of ASZ is about 820 HV. According to the microstructure of ASZ, the peak hardness in this zone is due to the fact that the eutectic-type structure contains hard brittle nickel boride. Region II corresponds to ISZ. The average hardness of ISZ is 200 HV, which is lower than for BM. The interdiffusion of the alloying elements between the joint region and the base metal determines the hardness of ISZ. The low hardness of ISZ can be attributed to an insufficient diffusion of the alloying

(a)

(b)
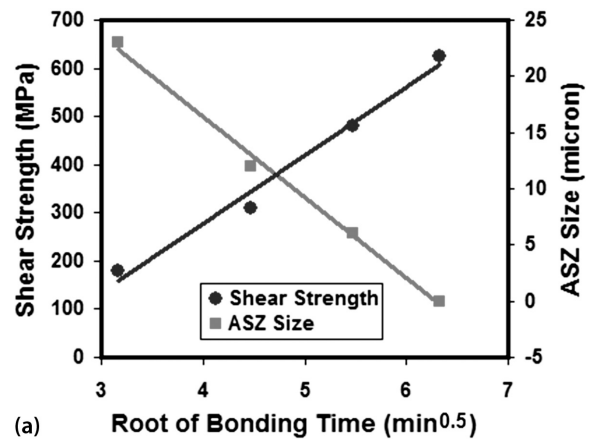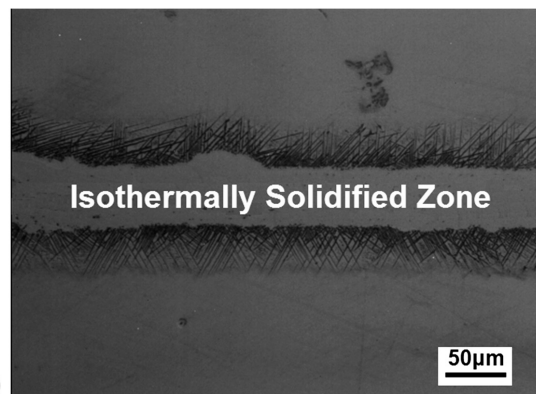
Figure 7: a) ASZ size and shear strength versus square root of bonding time, b) microstructure of the joint region after the completion of isothermal solidification at 1100 °C for 40 min

Slika 7: a) Velikost ASZ in strižna sila v odvisnosti od kvadratnega korena časa vezanja, b) mikrostruktura področja spoja po končanem izotermnem strjevanju pri 1100 °C in času 40 min

elements such as Nb, Mo, Cr, Al and Ti. The amounts of Nb, Mo, Cr, Al and Ti in ISZ (**Table 2**) are lower than those found in BM (**Table 1**). Region III corresponds to DAZ. The average hardness of DAZ is 420 HV, which can be related to boride precipitates. Region IV corresponds to the base metal.

3.2 Effect of the bonding time on the microstructure and hardness characteristics

A joint microstructure depends on the elemental interdiffusion between the base metal and the joint region, which in turn is governed by the bonding time. The average ASZ size was measured and plotted against the square root of the bonding time (**Figure 7a**). As can be seen, there is a linear relation between the ASZ size and the square root of the bonding time. According to Fick's second law,[29] the implication is that the formation of a gamma solid solution is a diffusion-controlled process. Indeed, in the case of the diffusion brazing of IN718/Ni-Cr-B/IN718, the isothermal solidification process is controlled by the formation and growth of the γ-solid solution, which is governed by the B diffusion in the base metal. An increase in the bonding time reduces the volume fraction of the eutectic-type microconstituent in the joint centerline. When the bonding time increased to 40 min, no eutectic microconstituent was observed in the bond region (**Figure 7b**). Therefore, it is concluded that the holding time of 40 min at 1100 °C is sufficient for an isothermal solidification completion.

The effect of isothermal solidification on the hardness profile is also superimposed in **Figure 6**. Since the isothermal solidification eliminates the eutectic-type microconstituent, it is not surprising that the peak hardness in the joint centerline is not present. However, the completion of isothermal solidification does not influence the peak hardness in DAZ. This is due to the fact that boride precipitates in DAZ are still stable even after the isothermal-solidification completion.

3.3 Effect of the bonding time on the shear strength

The effect of the bonding time on the shear strength of the TLP joints is shown in **Figure 7a**. It can be seen that an increase in the bonding time increases the joint shear strength. As can be seen, the shear strength of the bonds made at 1100 °C for 10 min is the lowest. According to Figure 7a there is an inverse relation between the joint shear strength and the ASZ size. When the bonding time is increased up to 20 min, the joint shear strength increases to 310 MPa. With a further increase in the bonding time up to 30 min, the joint shear strength increases to 480 MPa. This can be related to the decrease in the ASZ size. Therefore, it can be deduced that in the bonding condition, in which the isothermal solidification is not completed, the extent of the eutectic constituent (ASZ) is the controlling factor of the joint strength. A high hardness of the eutectic products (**Figure 6**) is coupled with the fact that the boride phases form the interlinked network provide a metallurgical notch, which significantly decreases the load-carrying capacity of the joint. Therefore, it is necessary to eliminate the eutectic products in order to improve the strength of the joints. In the bonding time of 40 min at 1100 °C, when the eutectic products are completely removed, the bonds with the shear strength of 625 MPa were achieved.

4 CONCLUSIONS

The joining of the as-cast IN718 nickel-based superalloy was conducted through the TLP bonding using Ni-15.2Cr-4B (in mass fractions, %) at the bonding temperature of 1100 °C. The following conclusions can be drawn from this study:

1. The solidification mechanism of the liquid phase is controlled with the bonding time. When the bonding time is lower than the critical value (40 min for the present system), isothermal solidification is not completed at the bonding temperature and the remaining liquid is transformed into a eutectic-type microconstituent made up of Ni-rich boride, Cr-rich boride and a eutectic-gamma solid solution.
2. A complete isothermal solidification which resulted in the formation of an intermetallic-free joint centerline occurred after the holding time of 40 min at the bonding temperature of 1100 °C.
3. Extensive Cr-Mo-Nb-based boride precipitates were observed in DAZ. These precipitates were stable even after the completion of isothermal solidification.
4. It has been shown that the bonding time has a significant impact on the joint mechanical properties in terms of hardness distribution and shear strength. An increase in the bonding time increased the shear strength of the joint due to a decrease in the width of the eutectic-type microconstituents.
5. It was found that there is an inverse relation between the width of a eutectic-type microconstituent (i.e., ASZ) and the shear strength of the TLP bonded IN718.

5 REFERENCES

[1] A. Milosavljevic, S. Petronic, S. Polic-Radovanovic, J. Babic, D. Bajic, The influence of the heat treatment regime on a fracture surface of nickel-based superalloys, Mater. Tehnol., 46 (**2012**) 4, 411–417
[2] R. Sunulahpašić, M. Oruć, M. Hadžalić, M. Rimac, Optimization of the mechanical properties of the superalloy Nimonic 80A, Mater. Tehnol., 46 (**2012**) 3, 263–267

³ A. Semenov, S. Semenov, A. Nazarenko, L. Getsov, Computer simulation of fatigue, creep and thermal-fatigue cracks propagation in gas-turbine blades, Mater. Tehnol., 46 (**2012**) 3, 197–203

⁴ B. Rivaux, X. Cao, M. Jahazi, J. Cuddy, A. Birur, Effect of pre- and post-weld heat treatment on metallurgical and tensile properties of Inconel 718 alloy butt joints welded using 4 kW Nd:YAG laser, J. Mater. Sci., 44 (**2009**), 4557–4571

⁵ A. C. Yeh, K. W. Lu, C. M. Kuo, H. Y. Bor, C. N. Wei, Effect of serrated grain boundaries on the creep property of Inconel 718 superalloy, Mater. Sci. Eng. A, 530 (**2011**), 525–529

⁶ M. Pouranvari, A. Ekrami, A. H. Ekrami, Microstructure development during transient liquid phase bonding of GTD-111 nickel-based superalloy, J. Alloys Comp., 461 (**2008**), 641–647

⁷ J. H. G. Matthij, Role of brazing in repair of superalloy components-advantages and limitations, Mater. Sci. Technol., 1 (**1985**), 608–612

⁸ A. Rabinkin, Brazing with (NiCoCr)-B-Si amorphous brazing filler metals: Alloys, processing, joint structure, properties, applications, Sci. Technol. Weld. Joining, 9 (**2004**), 181–199

⁹ S. K. Tung, L. C. Lim, M. O. Lai, Solidification phenomena in nickel base brazes containing boron and silicon, Scripta Mater., 34 (**1996**), 125–133

¹⁰ N. R. Philips, C. G. Levi, A. G. Evans, Mechanisms of Microstructure Evolution in an Austenitic Stainless Steel Bond Generated Using a Quaternary Braze Alloy, Metall. Mater. Trans. A, 39 (**2008**), 142–9

¹¹ A. Sakamoto, C. Fujiwara, T. Hattori, S. Sakai, Optimizing processing variables in high-temperature brazing with nickel-based filler metals, Weld. J., 68 (**1989**), 63–71

¹² M. A. Arafin, M. Medraj, D. P. Turner, P. Bocher, Transient liquid phase bonding of Inconel 718 and Inconel 625 with BNi-2: Modeling and experimental investigations, Mater. Sci. Eng. A, 447 (**2007**), 125–133

¹³ M. Pouranvari, A. Ekrami, A. H. Kokabi, Microstructure-properties relationship of TLP-bonded GTD-111 nickel-base superalloy, Mater. Sci. Eng. A, 490 (**2008**), 229–234

¹⁴ O. A. Ojo, N. L. Richards, M. C. Charturvedi, Effect of gap size and process parameters on diffusion brazing of Inconel 738, Sci. Technol. Weld. Joining, 9 (**2004**), 209–220

¹⁵ D. S. Duvall, W. A. Owczarski, D. F. Paulonis, TLP Bonding: A new method for joining jeat resistant alloys, Weld. J., 53 (**1974**), 203–214

¹⁶ R. Thambury, W. Wallace, J. A. Goldak, Post weld heat treatment cracking in superalloys, Int. Met. Rev., 28 (**1983**), 1–22

¹⁷ N. L. Richards, X. Huang, M. C. Chaturvedi, Heat affected zone cracking in cast inconel 718, Mater. Charact., 28 (**1992**), 179–87

¹⁸ C. H. Radhakrishna, K. P. Rao, The formation and control of Laves phase in superalloy 718 welds, J. Mater. Sci., 32 (**1997**), 1977–1984

¹⁹ G. D. J. Ram, A. V. Reddy, K. P. Rao, G. M. Reddy, Control of Laves phase in Inconel 718 GTA welds with current pulsing, Sci. Technol. Weld. Joining, 9 (**2004**), 390–398

²⁰ M. Pouranvari, A. Ekrami, A. H. Kokabi, Effect of bonding temperature on microstructure development during TLP bonding of a nickel base superalloy, J. Alloys Comp., 469 (**2009**), 270–275

²¹ W. F. Gale, D. A. Butts, Transient liquid phase bonding, Sci. Technol. Weld. Joining, 9 (**2004**), 283–300

²² O. A. Idowu, N. L. Richards, M. C. Chaturvedi, Effect of bonding temperature on isothermal solidification rate during transient liquid phase bonding of Inconel 738LC superalloy, Mater. Sci. Eng. A, 397 (**2005**), 98–112

²³ F. Jalilian, M. Jahazi, R. A. L. Drew, Microstructural evolution during transient liquid phase bonding of Inconel 617 using Ni-Si-B filler metal, Mater. Sci. Eng. A, 447 (**2007**), 125–33

²⁴ M. Pouranvari, A. Ekrami, A. H. Kokabi, Microstructure-properties relationship of TLP-bonded GTD-111 nickel-base superalloy, Materials Science and Engineering A, 490 (**2008**), 229–34

²⁵ D. A. Butts, Transient liquid phase bonding of a third generation gamma-titanium aluminium alloy-Gamma Met PX, PhD thesis, Auburn University, 2005

²⁶ T. B. Massalski (ed.), Binary alloy phase diagrams, ASM, Metals Park, OH 1986

²⁷ K. Ohsasa, T. Shinmura, T. Narita, Isothermal solidification behavior during the transient liquid phase bonding process of nickel using binary filler metals, J. Phase Equil., 20 (**1999**), 199–206

²⁸ W. F. Gale, E. R. Wallach, Microstructural development in transient liquid-phase bonding, Metall. Trans. A, 22 (**1991**), 2451–2457

²⁹ J. Crank, The Mathematics of Diffusion, 2nd ed., Oxford University Press, Oxford, United Kingdom 1975